ChemComm

NH₃ treatment of TiO₂ nanotubes: from N-doping to semimetallic conductivity†

Shaeel A. Al-Thabaiti,[a] Robert Hahn,[b] Ning Liu,[b] Robin Kirchgeorg,[b] Seulgi So,[b] Patrik Schmuki,*[ab] Sulaiman N. Basahel[a] and Salem M. Bawaked[a]

In the present work we show that a suitable high temperature ammonia treatment allows for the conversion of single-walled TiO₂ nanotube arrays not only to a N-doped photoactive anatase material (which is already well established), but even further into fully functional titanium nitride (TiN) tubular structures that exhibit semimetallic conductivity.

Several functional features have made TiO_2 one of the most studied compounds in materials science over the past few decades. This unique role is, to a large extent, due to its semiconductive nature, which is key to the successful use of the material in photocatalysis[1–3] and solar cells.[4,5] In these applications, the optical properties – namely, a band-gap of 3.0–3.2 eV and the energetic location of the band edge positions relative to the redox potential of the environment – are crucial. TiO_2 has the potential for an even wider range of applications including as an electrode for Li-intercalation,[6] a support in methanol fuel cells[7] or in supercapacitors,[8] but such uses as an electrode material are hampered by the moderate electron conductivity of TiO_2.[9] In this context, a conversion of the material to a semimetallic nitride[10–12] may be highly promising because, in such electrode configurations, electron transport through the material to the back contact is of utmost importance for the performance of the devices. A fact common to photoelectrochemical and electrode applications is that nanostructured electrodes are beneficial, as they provide a large surface area for adsorption, reaction, and intercalation processes. Nanostructured electrodes are classically prepared from TiO_2 nanoparticles compacted onto a metallic or transparent-conducting-oxide (TCO) back contact. However, in recent years 1D nanostructures have attracted wider interest, as their morphology provides defined geometries that allow for ideal ion and charge transport pathways, *e.g.* directional electron transport to the back contact and highly

defined ion diffusion pathways. One of the most straightforward approaches used to create defined 3D titania electrodes is the formation of ordered TiO_2 nanotube arrays *via* the self-ordering anodic oxidation of Ti metal sheets.[13,14]

In order to improve the optical and electronic properties of nanostructured TiO_2 electrodes, a large amount of effort in past and current research has been dedicated to doping,[15,16] or band-gap engineering of the materials using a wide range of transition metals such as vanadium, cerium, manganese and nickel,[17–21] or nonmetals such as C, N and S.[15,16,22,23] At present, the most successful approach for varying the optical and electrical properties remains N-doping, which can be conducted using various techniques.[24] At low to medium nitrogen concentrations, most reports describe the formation of N-substitutional states close to the valence band of TiO_2. This has been successfully used to narrow the optical absorption edge and cause the well-established activation of TiO_2 in the visible range of the optical spectrum.

Nitrogen doping can be achieved *via* heating TiO_2 in NH_3 (at several hundred °C), and such an approach has been used successfully to create N-doped TiO_2 nanotube arrays.[24,25] Nevertheless, a drastic improvement in conductivity can be achieved by full conversion of TiO_2 to titanium nitride.[26,27] For TiO_2 particles this can be achieved using a heat treatment in NH_3 at much higher temperatures (typically >1000 °C)[28–30] with a conversion sequence as proposed (for example) by Z. Zhang *et al.*[31]

Nevertheless, our own preliminary efforts have revealed that a key problem in the conversion of TiO_2 nanotube layers to conductive nitride tubes is that conventional TiO_2 nanotube structures decay at elevated temperatures (due to sintering or collapse), as shown in ESI,† Fig. S1. These 'classic' tubes contain a large amount of carbon,[32,33] which leads to contamination of the walls and mechanical weakness under the harsh high temperature reduction treatment in ammonia gas.

In the present work we show that this structural decay can be overcome using so-called single walled nanotubes (Fig. 1 and Fig. S2, ESI†). This allows for the successfully conversion of the TiO_2 nanotube arrays into aligned Ti–nitride nanotubular arrays that maintain a defined tubular geometry, are well

[a] *Department of Chemistry, King Abdulaziz University, Jeddah, Saudi Arabia.*
 E-mail: schmuki@ww.uni-erlangen.de
[b] *Department of Materials Science and Engineering, WW4-LKO,*
 University of Erlangen-Nuremberg, Martensstrasse 7, D-91058 Erlangen, Germany
† Electronic supplementary information (ESI) available. See DOI: 10.1039/c4cc02069c
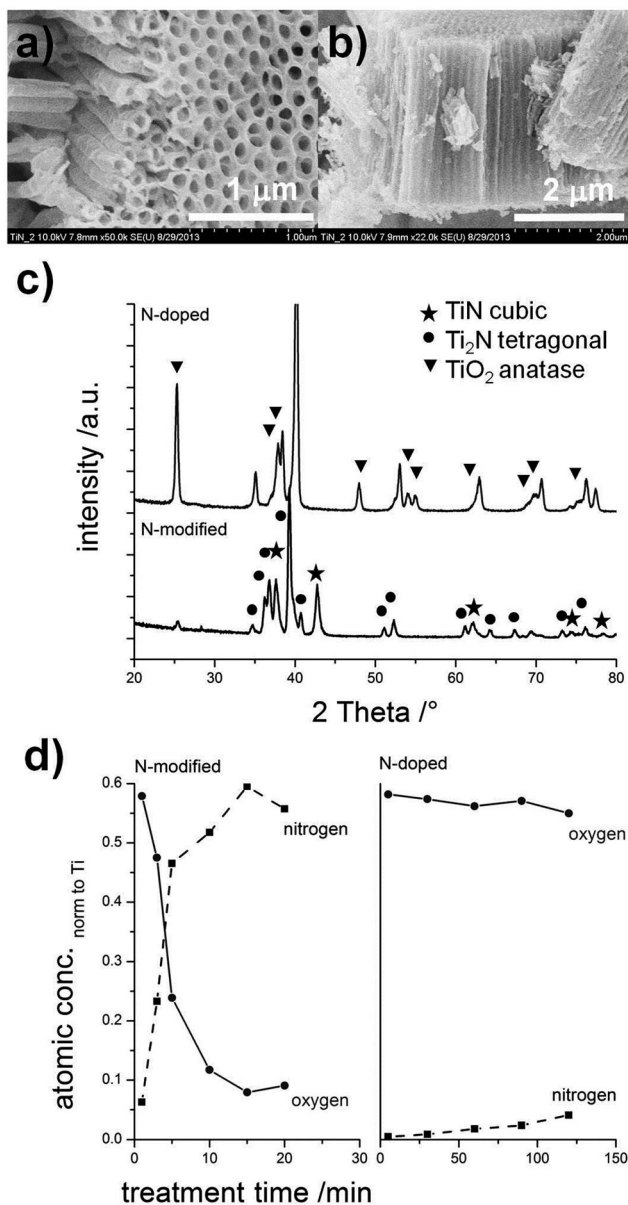
Fig. 1 SEM images – top view (a) and cross section (b) – of the nanotubes after thermal treatment in ammonia at 900 °C for 10 minutes. (c) Shows XRD results for the ammonia treated tubes (converted to nitride) compared to N-doped TiO$_2$ nanotubes. (d) EDX data for nanotube layers thermally treated in an ammonia atmosphere at 450 °C (N-doped) and 900 °C (N-converted) for different treatment times.

anchored onto the substrate and, most importantly, show semimetallic conductivity.

Fig. 1a and b and ESI,† Fig. S2 show the morphology of the TiO$_2$ nanotube layers produced either with a common ethylene glycol (EG) based-electrolyte to form a conventional double wall morphology (see ESI,† Fig. S2) or by using anodization in an EG–DMSO electrolyte to form a single wall morphology,[32] as described in ESI,† Fig. S2. From the SEM images in Fig. 1 and Fig. S1 (ESI†) it is clear that a very different morphological stability is observed for the heat treatment in NH$_3$ at 900 °C. In the case of the double walled structure observed in Fig. S1

(ESI†), the collapse of the tubes is likely to be associated with the inner (contaminated) tube wall and its partial decomposition during sintering.[32,33] Clearly, the single wall tubes in Fig. 1 (that consist only of the outer shell) maintain their diameter, length and overall appearance.

Fig. 1c and d show XRD and XPS characterization for two N-modified single-wall samples. In the first sample the tubes were N-doped using a treatment in NH$_3$ at 450 °C; in the second, the tube layers were treated at 900 °C in NH$_3$. The XRD data for the first N-doped sample reveals only the typical peaks of anatase, while the higher temperature sample shows a conversion to two forms of titanium nitride. In the XRD pattern, clear peaks for cubic TiN and tetragonal Ti$_2$N can be identified. In this case, no trace of any peaks corresponding to an oxide-phase can be detected in the XRD pattern. Fig. 1d shows a quantitative evaluation of the nitrogen and oxygen content derived from XPS data taken from a series of samples annealed in NH$_3$ at 900 °C (conversion) and 450 °C (doping) for different treatment times.

Fig. 2 shows the XPS spectra of the Ti2p and N1s regions measured for a fully converted and a nitrogen doped sample. The most distinct difference is that, for the doped sample, the typical TiO$_2$ signature is still apparent in the Ti2p region, whereas the spectrum of the nitrated sample shows distinct additional peaks at 462 eV and 465 eV, which are typical of Ti–N compounds. The N1s region for both samples shows a peak at 396 eV that is commonly ascribed to Ti–N bonds – this peak is much stronger for the fully nitrated sample in comparison to the doped material. The additional peak at 398 eV can be ascribed to TiON,[34] the peak at ≈ 400 eV to adsorbed N$_2$ and the peak at ≈ 402 eV to adsorbed NH$_3$ or amine species adsorbed onto the material surface.

2-Point solid state measurements (Fig. 3a) using an evaporated Au-top contact conducted on the TiO$_2$ nanotube layers show a strong difference in the I–V behavior between the different NH$_3$-treated nanotubes. Non-NH$_3$-treated (anatase) nanotube layers show typical n-type semiconductive behavior, with current passing behavior under negative bias and blocking behavior under positive bias. Conventional nitrogen doping increases the overall conductivity, i.e. the reverse and forward bias show considerable increases. However, conversion to nitride yields fully symmetrical ohmic behavior with a conductivity of approx. 10^5 S m^{-1}, i.e. a value comparable to typical semi-metals,[35] and characteristics in line with the literature.[26,27]
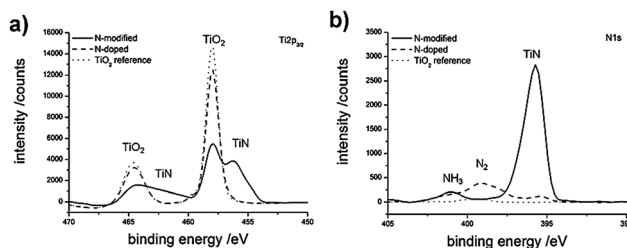

Fig. 2 XPS spectra showing the Ti2p and N1s peaks of the nanotubes converted to nitride compared to N-doped TiO$_2$ nanotubes and (non-doped) anatase TiO$_2$ nanotubes.
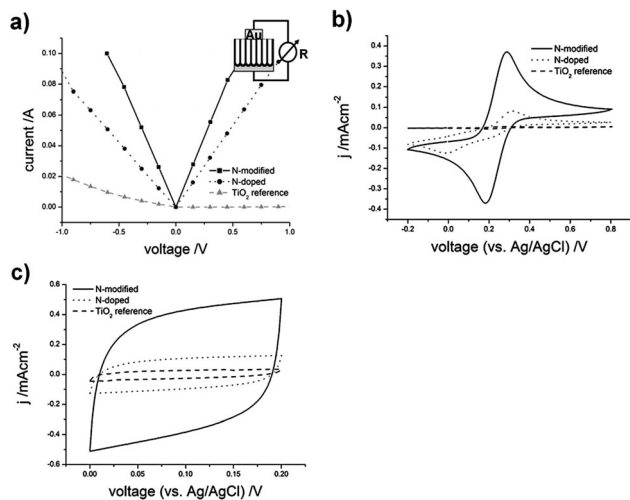
Fig. 3 I–V characteristics from 2-point solid state measurements of the nanotubes converted to nitride compared with N-doped layers and (non-doped) anatase TiO_2 nanotube layers (a) and electrochemical characterization using cyclic voltammetry of the nanotubes converted to nitride compared with the N-doped layers and (non-doped) anatase TiO_2 nanotube layers in (b) 5 mM $Fe(CN)_6^{-2/-3}$ solution and (c) 0.1 M HCl.
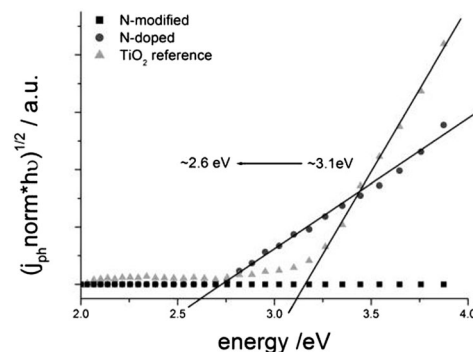

Fig. 4 Band-gap determination from photocurrent spectra for the nanotubes converted to nitride, N-doped layers and (non-doped) anatase TiO_2 nanotube layers.

Such high conductivity values could enable the use of the material as a 'conductive' nanotube electrode as can easily be seen, not only from the conductivity measurements in Fig. 3a, but also from the cyclic voltammograms in Fig. 3b. In Fig. 3b, the CVs for the different electrodes were acquired in a $Fe(CN)_6^{2-/3-}$ solution. In contrast to the pure TiO_2 or N-doped TiO_2 electrodes, for the Ti–nitride sample, oxidation and reduction peaks are obtained comparable to typical noble metal electrodes. Moreover, an evaluation of the material under fast scanning and using a simple 0.1 M HCl electrolyte (Fig. 3c) shows a larger difference between the nitrided sample and the doped or native material. The nitrided electrode exhibits the obvious featureless shape of a double layer capacitor with a specific capacitance of 100 F g^{-1} at 100 mV s^{-1} – indicating a fast and high capacitance response for these nanostructured conductive electrodes (in fact, the current is higher than that reported under identical conditions for the best tube modification[36]). This suggests that while the semiconductive materials capacitance values are partially dominated by their space charge layers, for the nitrided sample a metallic behavior (dominated by the Helmholtz layer) is observed.

The entirely different nature of nitrogen-doping and conversion to a nitride is also evident when the photoresponse of the electrodes is investigated. Fig. 4 shows the photocurrent spectra measured in a 0.1 M Na_2SO_4 electrolyte at 500 mV Ag/AgCl. For anatase TiO_2 a band-gap of 3.1 eV is obtained, which is typical of an indirect electron transition in a semiconductor. The N-doped sample still shows a distinct semiconductive photoresponse with a band-gap of ≈ 2.6 eV (which is in line with the previous literature on N-doped TiO_2[24,25]). In contrast, the material converted to Ti–nitride shows no measurable photoresponse – as would be expected from a metal.[26,27]

In summary, in the present work we have shown that ammonia-based heat treatments of TiO_2 nanotubes can not only be used in a classical approach to nitrogen dope the material (and, thus, impart visible light semiconductive behavior), but also – under suitable conditions – to create arrays of Ti–nitride tubes that exhibit semimetallic conductivity.

The key to obtaining successful conversion is not only using an optimized NH_3 treatment, but, most importantly, the use of 'single-walled' TiO_2 nanotubes that are found to be more thermally robust than 'classic' nanotube layers.

The resulting conductive nanotube-arrays may potentially be used for a variety of applications such as highly defined electrodes in electrochemical sensors or as supercapacitor scaffolds.

Notes and references

1 A. L. Linsebigler, G. Lu and J. T. Yates, Chem. Rev., 1995, 95, 735.
2 A. Fujishima and K. Honda, Nature, 1972, 238, 37.
3 M. R. Hoffmann, S. T. Martin, W. Cho and D. W. Bahnemann, Chem. Rev., 1995, 95, 69.
4 B. O. Regan and M. Graetzel, Nature, 1991, 353, 737.
5 M. Graetzel, Nature, 2001, 414, 338.
6 W. Wei, G. Oltean, C. W. Tai, K. Edström, F. Björeforsa and L. Nyholma, J. Mater. Chem. A, 2013, 1, 8160.
7 J. M. Macak, F. Schmidt-Stein and P. Schmuki, Electrochem. Commun., 2007, 9, 1783.
8 Y. Yang, D. Kim, M. Yang and P. Schmuki, Chem. Commun., 2011, 47, 7746.
9 S. So and P. Schmuki, Angew. Chem., Int. Ed., 2013, 52, 7933.
10 J. G. Li, Q. H. Zhang, J. Sun and W. Ling, J. Inorg. Mater., 2003, 18, 765.
11 S. Kawano, J. Takahashi and S. Shimada, J. Am. Ceram. Soc., 2003, 86, 1609.
12 L. E. Toth, Transition metal carbides and nitrides, Academic Press, New York, 1971.
13 P. Roy, S. Berger and P. Schmuki, Angew. Chem., Int. Ed., 2011, 50, 2904.
14 D. Kowalski, D. Kim and P. Schmuki, Nano Today, 2013, 8, 235.
15 R. Asahi, T. Morikawa, T. Ohwaki, K. Aoki and Y. Taga, Science, 2001, 293, 269.
16 H. Wang and J. P. Lewis, J. Phys.: Condens. Matter, 2006, 18, 421.

17 T. Umebayashi, T. Yamaki, H. Itoh and K. Asai, *J. Phys. Chem. Solids*, 2002, **63**, 1909.

18 J. Osorio-Guillen, S. Lany and A. Zunger, *Phys. Rev. Lett.*, 2008, **100**, 036601.

19 Y. Wang and D. J. Doren, *Solid State Commun.*, 2005, **136**, 142.

20 C. D. Valentin, G. Pacchioni, H. Onishi and A. Kudo, *Chem. Phys. Lett.*, 2009, **469**, 166.

21 G. Shao, *J. Phys. Chem. C*, 2009, **113**, 6800.

22 K. Yang, Y. Dai, B. Huang and M.-H. Whangbo, *J. Phys. Chem. C*, 2009, **113**, 2624.

23 K. Yang, Y. Dai and B. Huang, *J. Phys. Chem. C*, 2007, **111**, 18985.

24 I. Paramasivam, H. Jha, N. Liu and P. Schmuki, *Small*, 2012, **8**, 3073.

25 R. P. Vitiello, J. Macak, A. Ghicov, H. Tsuchiya, L. F. P. Dick and P. Schmuki, *Electrochem. Commun.*, 2006, **8**, 544.

26 V. Ern and A. C. Switendick, *Phys. Rev.*, 1965, **137**(6A), A1927.

27 A. Münster, *Angew. Chem.*, 1957, **69**(9), 281.

28 J. G. Li, Q. H. Zhang, J. Sun and W. Ling, *J. Inorg. Mater.*, 2003, **18**, 765.

29 S. Kawano, J. Takahashi and S. Shimada, *J. Am. Ceram. Soc.*, 2003, **86**, 1609.

30 L. E. Toth, *Transition metal carbides and nitrides*, Academic Press, New York, 1971.

31 Z. Zhang, J. B. M. Goodall, D. J. Morgan, S. Brown, R. J. H. Clark, J. C. Knowles, N. J. Mordand, J. R. G. Evans, A. F. Carley, M. Bowker and J. A. Darr, *J. Eur. Ceram. Soc.*, 2009, **29**, 2343.

32 H. Mirabolghasemi, N. Liu, K. Lee and P. Schmuki, *Chem. Commun.*, 2013, **49**, 2067.

33 S. P. Albu, A. Ghicov, S. Aldabergenova, P. Drechsel, D. LeClere, G. E. Thompson, J. M. Macak and P. Schmuki, *Adv. Mater.*, 2008, **20**, 4135.

34 X. Chen and C. Burda, *J. Phys. Chem. B*, 2004, **108**, 15446.

35 L. Forro, O. Chauvet, D. Emin, L. Zuppiroli, H. Berger and F. Levy, *J. Appl. Phys.*, 1994, **75**, 633.

36 X. Lu, G. Wang, T. Zhai, M. Yu, J. Gan, Y. Tong and Y. Li, *Nano Lett.*, 2012, **12**, 1690.